ELSEVIER

Journal of Nuclear Materials 289 (2001) 48–51

journal of nuclear materials

www.elsevier.nl/locate/jnucmat

XPS characterization of beryllium carbide thin films formed via plasma deposition

Yixiang Xie *, Nicholas C. Morosoff, William J. James

Electronic Materials Applied Research Center, Materials Research Center, University of Missouri-Rolla, Rolla, MO 65401, USA

Abstract

Beryllium carbide thin films were deposited onto selected substrates. Such films may serve as inertial confinement fusion target coatings and have potential for magnetic fusion reactors. The films were characterized by X-ray photoelectron spectroscopy (XPS) and four-point probe electrical conductivity measurement (FPPM) among others. XPS analyses established that: (1) beryllium carbide is the dominant chemical composition; (2) atomic Be in excess of stoichiometric carbide is dispersed within a carbide matrix and small amount of carbon is present; (3) increasing charging shifts in the XPS spectra with decreasing Be content suggests higher electrical resistivity in these films which is confirmed by FPPM of film electrical conductivity.

1. Introduction

In a previous paper [1], we described the synthesis, chemical and thermal characterizations of a beryllium carbide composite for the ICF target capsule outermost coating, in general. Although Auger electron spectroscopy (AES) and X-ray diffraction patterns provide information of chemical composition, XPS is an important tool to identify chemical states of each element in the materials. X-ray photoelectron spectroscopy (XPS) or electron spectroscopy for chemical analysis (ESCA) is a technique popularly used in surface analysis [2–5]. In XPS, an X-ray photon beam strikes a surface and excites the inner shell electrons of the surface and near surface atoms in the material. The binding energies of the excited electrons related to the incident photon energy and the measured kinetic energy are used to identify the elements except for hydrogen. X-rays have less of a charging effect than do electron beams. XPS is a better choice for examining the surfaces of insulating materials because less charging occurs than does with AES. The XPS spectrum is a plot of the number of electrons per unit energy $N(E)$ vs. the binding energy. The peak areas and sensitivity factors of the detected elements are used to determine the concentration of the elements in the surface materials. The effective atomic potential is affected by the chemical state of the element which further affects the binding energy of the inner shell electron, i.e., a change of the chemical state of an element will cause a shift in the binding energy corresponding to the element [3,5,6], thus XPS provides information on chemical states. Spin–orbit splitting may cause peak-splitting corresponding to chemical states [6–8], and different effects of shift (splitting) may occur due to the nonmonochromatic nature of the X-rays, the photoelectron process itself (shake up, shake off), unpaired electrons in the valence levels, and plasmon satellites [7–9]. Electrons from flood guns to reduce charging may cause sample decomposition and it is possible that the sample may charge nonuniformly, enough to give rise to multiple peaks in the XPS spectrum which mislead one to believe that there exist multiple chemical states [6]. XPS can also distinguish amorphous carbon, diamond and graphite [10–14]. The charging effect of a nonconducting sample on the binding energies will move the peaks, corresponding to different elements, to higher levels. However, the binding energy differences are independent of sample charging [6]. This means that the absolute binding energy for a certain chemical state of a given element does not exist but a relative one does.

* Corresponding author. Tel.: +1-573 341 4405; fax: +1-573 341 6151.

E-mail address: xie@umr.edu (Y. Xie).

0022-3115/01/$ - see front matter
PII: S0022-3115(00)00682-6

A typical lateral resolution of XPS is about several millimeter [5], which is much larger than that of AES, 500 nm to 5 mm. To obtain a depth profile of a surface sample from XPS, the ion sputtering beam has to sputter a larger area than in AES. The relatively slow depth sputtering rate of XPS often results in oxygen contamination of the sample surface due to O_2 and H_2O adsorption especially under poor vacuum conditions [5,15–17], and in the case of oxygen sensitive samples. At 10^{-4} Pa ($\sim 7.5 \times 10^{-7}$ Torr), the contamination rate on a surface is one monolayer/second [5] assuming a sticking coefficient of 1. Due to its slow sputtering rate, XPS is not frequently used for depth profiling [3,5].

Thermal conductivity is an important parameter for the application. Thermal energy is carried through a solid material by electrons and phonons which are quanta of energy of elastic (sound) waves [18,19]. Therefore, the electrical conductivity or resistivity of a material is an important index to understand the contribution of electrons to the thermal conductivity of the material. Electrical resistivities of thin films may be determined by four-point probe measurements (FPPMs) [20,21]. Four tips (probes) contact or penetrate a thin film surface (depending on the relative hardness of the tips and the film material), at four points which form a parallelogram. A current (I, ampere) is applied between a pair of diagonal tips, the electrical potential (V, volt) is measured. The electrical resistivity ρ of the film is expressed as

$$\rho = \pi \times V \times t/(\ln 2 \times I),$$

where t is the film thickness (cm).

2. Experimental

Films deposited on 1×1 cm^2 aluminum foil substrates were analyzed with a model 548 X-ray photoelectron spectrometer made by Physical Electronics after 60 min of sputtering at a rate of 50 Å/min. The films for XPS and for AES analyses were prepared simultaneously and the substrates were located in the region which ensured a reasonable compositional uniformity of the film. The X-ray source of the spectrometer is Mg K_a (1253.6 eV). Typical operation conditions were: X-ray gun, 10 KV, 40 mA; pass energy, 50 eV, chamber pressure, 5×10^{-7} to 5×10^{-8} Torr. A computer curve fitting routine program was used for determining the chemical states.

The electrical conductivity of thin films deposited on glass substrates were measured with a four-point probe made by Alessi, using osmium soft tips and equipped with a Keithley 220 current source and a 610c electrometer. To compare the conductivities of films deposited with and without post annealing, films of Group 1 were also deposited on tantalum foil substrates and prepared as above. Two samples were annealed at 1000°C for five days under high purity argon. Both annealed and unannealed samples were measured using the four-point probe.

3. Results and Discussion

Low oxygen-containing Be–C films have been made by magnetron sputtering of beryllium into a methane plasma. Elemental compositions can be controlled by varying the flow rate ratio of the reactive gas methane to the sputtering media. The results of AES for the films are shown in Table 1 [1]. Films were repeatedly made and analyzed under each group conditions and the results were in good agreement.

AES analysis established the beryllium, carbon and oxygen ratios in the films deposited by reactive magnetron sputtering. Furthermore the spectra evidenced the presence of Be_2C [1]. All this suggested that XPS analysis should be carried out as it would provide further information as to the compounds in the films. Table 2 gives the electron binding energy level in the element's inner shell for different chemical states. In most cases, XPS data are collected only from the top surfaces of samples. For beryllium-containing materials (beryllium is a strong oxygen getter), we chose to carry out the XPS analyses at an approximate depth of 300 nm. As discussed in the instruction. XPS data taken within a film via sputtering, may result in about a 10% deviation in each elemental concentration. However, XPS will still provide information on the majority of the chemical

Table 1
AES results of film compositions

Group no.	Flow rate ratio of methane/argon	Be (at.%)	C (at.%)	O (at.%)
1	0.1	74–76	23–25	0.1–2
2	0.15	64–65	31–33	2–3
3	0.2	61–63	33–36	2–3
4	0.25	56–58	35–39	2–4
5	0.3	45–52	46–53	1.3–2.5

Table 2
Binding energy (eV)

Be_{1s} [22]	111.5
Be_{1s} (BeO) [2]	114.1
Be_{1s} (Be_2C) [2]	112.4
C_{1s} (Be_2C) [2]	282.1
C_{1s} (miscellaneous)	284, diamond; 284.2 graphite [10–12]; 284.6 hydrocarbon [23]
O_{1s} [22]	543.1
O_{1s} (BeO) [23]	531.6

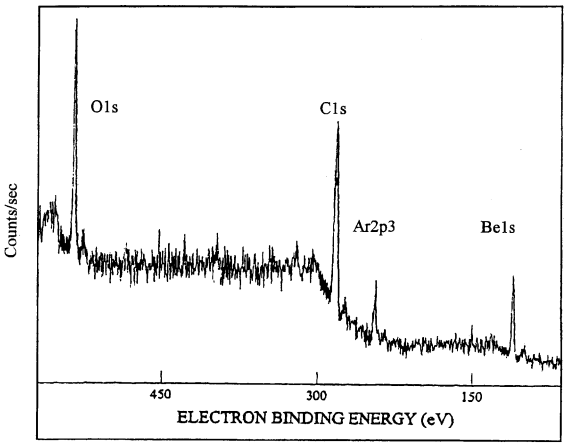

Fig. 1. Typical XPS spectrum.

states for each element present in the films. Fig. 1 is a typical XPS spectrum taken of a group one film after 60 min of sputtering, 300 nm from the top surface. The area under each peak combined with the sensitivity factor corresponding to the element was used to calculate the relative amount of the element in the film.

The deconvolution of the peaks in the XPS results in resolution of the elemental peaks to provide the chemical states and the relative amount of each element in that state. The peak separations typically are for samples deposited at flow rate ratio of methane to argon of 0.1, 0.2, and 0.25, respectively (Groups 1, 3, and 4). For Group 1, the Be_{1s} peak is separated into three symmetric peaks corresponding to Be at 111.3 eV, Be_2C at 112.1 eV, and BeO at 114 eV. Due to charging, all the peaks are shifted 0.1–0.3 eV lower than the values given in the literature. The C_{1s} peak at 281.8 is assigned to Be_2C, and the O_{1s} peak is assigned to BeO. For the same reason they shifted in the same direction from those in the literature as did the Be_{1s} peaks. The major chemical state is beryllium carbide, Be_2C in all three films. For Group 2, the Be_{1s} peak is also a combination of Be at 112 eV, Be_2C at 112.9 eV, and BeO at 114.6 eV with a 0.4–0.5 eV shift to higher levels than those in the literature. The same effect can be observed for the peaks of C_{1s} and O_{1s}. For the C_{1s} at 284.6 eV, close to that of graphite, and hydrocarbons. The O_{1s} peak at 532 eV is assigned to BeO. The major chemical state is Be_2C with graphitic/hydrocarbon carbon and atomic Be. The Group 4 for the carbon shows more graphitic carbon than that in Group 3, without the presence of atomic Be. However, Be_2C is still the dominant phase for both Be and C. For Group 4, the XPS peak separations of the film show a charging shift of 0.5–0.7 eV to higher levels than those given in the literature. The Be_{1s} electron binding energy shows a Be_2C peak at 113 eV, a BeO peak at 114.7 eV and the C_{1s} electron binding energy shows a Be_2C peak at 282.8 eV, a C peak at 285 eV, and an O_{1s} at 532.3 eV.

Table 3
Film electrical resistivity

Methane/Ar	Be (at.%)	C (at.%)	Resistivity (Ω cm)
0.1	75	24	3.4×10^2
0.2	62	35	6.7×10^3
0.3	49	50	9.0×10^5

XPS analyses give the film information as follows:

1. beryllium carbide is the major composition in the reactive magnetron sputter deposition films;
2. in the films containing Be in excess of stoichiometric Be_2C, atomic Be appears to exist, and in the films containing C in excess of stoichiometric beryllium carbide, graphitic and/or plasma-formed hydrocarbon polymers appear;
3. the larger charging shifts in the XPS spectra of the films with lower Be concentrations imply higher electrical resistivities in these films.

The contribution of the electrons to the thermal conductivity of a material is related to the electrical conductivity or resistivity of the solid material. Using the data of the four-point probe measurements of the 2 mm thick films deposited on glass substrates, the electrical resistivities of the films were determined and are shown in Table 3. According to the electrical resistivities and the compositions of the films in Table 3, the film electrical resistivity increases as the carbon concentration in the film increases, which is in agreement with XPS results where the higher the carbon concentration is in the film, the larger is the peak shift (stronger charging) due to the higher electrical resistivity of the film.

The reported bulk beryllium carbide electrical resistivity at 30°C is 6.3×10^{-2} Ω cm [24]. One of the reasons for the films having a higher electrical resistivity (or lower electrical conductivity) is grain boundary scattering. The small grain size (increases boundary length) reduces the electron and phonon flow in the solid materials. High temperature annealing can lead to increased crystallite size. The 5 mm thick films (Group 1) were deposited on tantalum foil. Two samples were annealed at 1000°C under argon gas protection for 5 days. The four-point probe was again used to measure the electrical resistivities of the annealed and unannealed films using soft osmium tips. The ratio of the electrical resistivities of the annealed films to those of the unannealed films is 5.3×10^{-4}. Annealing did decrease the film electrical resistivity (or increase the film electrical conductivity).

4. Conclusions

AES and XPS analyses provide strong evidence that beryllium carbide, Be_2C is the major phase in the films,

and that 'free' beryllium exists in the Be-rich films, and graphitic-like carbon in the C-rich films.

FPPM of the films result in electrical resistivities ranging from 3.4×10^2 to 9.0×10^5 Ω cm. The higher the carbon concentration in a film, the higher is the corresponding electrical resistivity of the film, which is in accordance with the observation that in XPS spectra, the higher the carbon concentration in a film, the larger is the peak shift in the spectrum. Annealing for 5 days at 1000°C decreases the electrical resistivity of a film, and possibly increases the thermal conductivity of the films.

References

[1] Y. Xie, R.B. Stephens, N.C. Morosoff, W.J. James, Fus. Technol. 38 (2000) 384.
[2] T.G. Nieh, J. Wadsworth, A. Joshi, Scr. Metall. 20 (1986) 87.
[3] D.A. Skoog, J.J. Leary, Principles of Instrumental Analysis, fourth ed., Sanders College Publishing, 1992, pp. 384, 393, 568, 571.
[4] J.L. Li, T.J. O'Keefe, W.J. James, Mater. Sci. Eng. B 7 (1990) 15.
[5] L-H. Lee, Adhesive Bonding, Plenum, London, 1991, pp. 144.
[6] N.H. Turner, The Handbook of Surface Imaging and Visualization, CRC, Boca Raton, 1995, pp. 33,63, 67, 875.
[7] A. Proctor, P.M.A. Sherwood, Anal. Chem. 54 (1982) 13.
[8] Briggs, M.P. Seah, Practical Surface Analysis, vol. 1, second ed., Wiley, Chichester, 1990, p. 128.
[9] W.F. Egelhoff Jr., Surf. Sci. Rep. 6 (1986) 253.
[10] F. Arezzo, N. Zacchetti, W. Zhu, J. Appl. Phys. 75 (10) (1994) 5375.
[11] F.R. McFeely, S.P. Kowalczyk, L. Lay, R.G. Carell, R.A. Pollak, D.A. Shirley, Phys. Rev. B 9 (1974) 5268.
[12] D.N. Belton, S.J. Harris, S.J. Schmieg, A.M. Weiner, T.A. Perry, Phys. Lett. 54 (1989) 416.
[13] T. Bruce, I. Bello, L.J. Huang, W.M. Land, M. High, V. Strnad, P. Panchhi, J. Appl. Phys. 76 (1) (1994) 552.
[14] W.M. Lau, L.J. Huang, I. Bello, Y.M. Yiu, S.T. Lee, J. Appl. Phys. 75 (1994) 3385.
[15] I.K. Schuller, C.M. Falco, Surf. Sci. 113 (1982) 443.
[16] B. Marchon, J. Carrazza, H. Heinemann, G.A. Somorjai, Carbon 26 (4) (1988) 507.
[17] M.J. Nowakowski, J.M. Vohs, D.A. Bonell, J. Am. Ceram. Soc. 76 (2) (1993) 279.
[18] K. Schroder, Electronic, Magnetic, and Thermal Properties, Marcell Dekker, 1980, p. 403.
[19] J. Ziman, Sci. Am. 217 (1967) 181.
[20] P. Herzig, J. Redinger, J. Chem. Phys. 82 (1985) 372.
[21] F.M. Smits, Bell Syst. Tech. J. (1958) 711.
[22] D.R. Lide, CRC Handbook of Chem. and Phys, 72 ed., CRC, Boca Raton, 1991–1992, pp. 4–44, 5–1, 5–6, 12–33, 12–119.
[23] R. Brusasco, S.A. Letts, P. Miller, M. Saculla, R. Cook, J. Vac. Sci. Technol. A 14 (3) (1996) 1019.
[24] J.F. Quick, Reactor Handbook, Materials, McGraw-Hill Book, New York, 1955, p. 95.